JOURNAL OF BACTERIOLOGY, Feb. 2007, p. 1013–1024 Vol. 189, No. 3
0021-9193/07/$08.00+0 doi:10.1128/JB.01328-06

Involvement of the *cynABDS* Operon and the CO_2-Concentrating Mechanism in the Light-Dependent Transport and Metabolism of Cyanate by Cyanobacteria[▽]

George S. Espie,* Farid Jalali, Tommy Tong, Natalie J. Zacal, and Anthony K.-C. So

Department of Biology, University of Toronto at Mississauga, Mississauga, Ontario L5L 1C6, Canada

Received 21 August 2006/Accepted 13 November 2006

The cyanobacteria *Synechococcus elongatus* strain PCC7942 and *Synechococcus* sp. strain UTEX625 decomposed exogenously supplied cyanate (NCO^-) to CO_2 and NH_3 through the action of a cytosolic cyanase which required HCO_3^- as a second substrate. The ability to metabolize NCO^- relied on three essential elements: proteins encoded by the *cynABDS* operon, the biophysical activity of the CO_2-concentrating mechanism (CCM), and light. Inactivation of *cynS*, encoding cyanase, and *cynA* yielded mutants unable to decompose cyanate. Furthermore, loss of CynA, the periplasmic binding protein of a multicomponent ABC-type transporter, resulted in loss of active cyanate transport. Competition experiments revealed that native transport systems for CO_2, HCO_3^-, NO_3^-, NO_2^-, Cl^-, PO_4^{2-}, and SO_4^{2-} did not contribute to the cellular flux of NCO^- and that CynABD did not contribute to the flux of these nutrients, implicating CynABD as a novel primary active NCO^- transporter. In the *S. elongatus* strain PCC7942 Δ*chpX* Δ*chpY* mutant that is defective in the full expression of the CCM, mass spectrometry revealed that the cellular rate of cyanate decomposition depended upon the size of the internal inorganic carbon (C_i) (HCO_3^- + CO_2) pool. Unlike wild-type cells, the rate of NCO^- decomposition by the Δ*chpX* Δ*chpY* mutant was severely depressed at low external C_i concentrations, indicating that the CCM was essential in providing HCO_3^- for cyanase under typical growth conditions. Light was required to activate and/or energize the active transport of both NCO^- and C_i. Putative *cynABDS* operons were identified in the genomes of diverse *Proteobacteria*, suggesting that CynABDS-mediated cyanate metabolism is not restricted to cyanobacteria.

Cyanate (NCO^-) metabolism has been studied extensively in *Escherichia coli* and to various degrees in a range of heterotrophic and autotrophic bacteria (references 4, 23, 41, and 50 and references therein). Key to this process is the enzyme cyanase (EC 4.2.1.104) which catalyzes the bicarbonate-dependent decomposition of cyanate to CO_2 and NH_3 (2, 15, 21, 47) according to the following reaction: $NCO^- + HCO_3^- + 2H^+ \rightarrow 2CO_2 + NH_3$. The net formation of CO_2 also means that cyanase cocatalyzes the irreversible dehydration of HCO_3^- (16).

Kinetic, isotopic, and X-ray crystallographic studies show that cyanase binds both NCO^- and HCO_3^- in the active site forming a dianion intermediate that enzymatically decarboxylates to CO_2 and carbamate (3, 28, 49). Spontaneous decarboxylation of the carbamate subsequently yields a second CO_2 and NH_3. Assimilation of cyanate-derived NH_3 and CO_2 then proceeds through conventional metabolic pathways providing a unique source of nitrogen (N) for growth in a variety of bacteria and a source of carbon (C) for autotrophic metabolism (7, 15, 30, 41, 50, 53).

In *E. coli*, the coexpression of carbonic anhydrase (CA) is vital to maintain ongoing cyanate metabolism (17, 23). Mutants lacking CA activity do not readily catalyze cyanate decomposition, are unable to grow with NCO^- as the sole N source, and are far more susceptible than wild-type cells to the toxic effects of cyanate itself on growth (18, 22–24). CA involvement is related to the absolute requirement by cyanase for HCO_3^- (rather than CO_2) as a substrate in the reaction. Physiological studies (17, 18, 22, 23) indicate that in the absence of CA, the CO_2 generated from cyanate decomposition diffuses out of cells faster than it can be hydrated nonenzymatically to HCO_3^-. This leads to a cellular depletion of HCO_3^- and cessation of cyanate metabolism through substrate deprivation. CA prevents this cellular depletion by trapping CO_2 and catalytically regenerating HCO_3^- within cells at a rate that is not limiting for cyanase.

Carbonic anhydrase, cyanase, and a hydrophobic protein designated as CynX are encoded by *cynT*, *cynS*, and *cynX* (4, 44), respectively, which are arranged in an operon in *E. coli*, ensuring the coordinated expression of the two enzymes required for cyanate decomposition. Expression of the *cynTSX* operon is induced by exogenous cyanate and positively regulated by CynR (45), a member of the LysR family of regulatory proteins. The *cynR* gene is located immediately upstream of the *cynTSX* operon but is transcribed in the opposite direction.

The photoautotrophic cyanobacterium *Synechococcus* sp. strain UTEX 625 also converts exogenous cyanate to CO_2 and NH_3 as described in the reaction above (30). Inhibitor studies (30) have shown that cyanate-derived NH_3 is rapidly incorporated by this cyanobacterium via the central nitrogen assimilation pathway, and it has recently been suggested that NCO^- can serve as the sole source of N for growth of the globally important marine cyanobacterium *Synechococcus* sp. strain WH8102 (35, 43). CO_2 arising from cyanate decomposition is also rapidly assimilated by *Synechococcus* sp. strain UTEX 625

* Corresponding author. Mailing address: Department of Biology, University of Toronto at Mississauga, 3359 Mississauga Rd., Mississauga, Ontario L5L 1C6, Canada. Phone: (905) 828-5380. Fax: (905) 828-3792. E-mail: espie@utm.utoronto.ca.

▽ Published ahead of print on 22 November 2006.

through the photosynthetic carbon reduction (Calvin) cycle. Consequently, NCO^- supports photosynthetic oxygen evolution (30). Biochemical and molecular studies have demonstrated cyanase activity in whole-cell extracts of *Synechococcus* sp. strain UTEX 625, *Synechococcus elongatus* strain PCC7942 and *Synechocystis* sp. strain PCC6803, which is absent from derived strains carrying engineered mutations within *cynS* homologs (19, 20, 30).

Unlike *E. coli*, the decomposition of exogenous cyanate by *Synechococcus* sp. strain UTEX625 is light dependent (30). The expression of *cynS* is not induced by exogenous cyanate, but it is negatively regulated by NH_3 and controlled by the global nitrogen regulator NtcA (19, 43). Sequence analysis also indicates that an operon similar to *E. coli cynTSX* is absent from the genomes of cyanobacteria examined to date. Although monocistronic *cynT* homologs have been identified and characterized as part of the CO_2-concentrating mechanism (CCM) of cyanobacteria (5, 39, 40), a corequirement for CA activity in cyanobacterial NCO^- decomposition has not been demonstrated. Instead, it has been proposed that the active HCO_3^- transport systems that normally provide inorganic carbon (C_i) ($[CO_2] + [HCO_3^-] + [CO_3^{2-}]$) for photosynthesis may fulfill the role that is played by CA in *E. coli* (30).

The ability of heterotrophs and autotrophs to utilize exogenous NCO^- as a source of N and C presumably relies upon the transport of this anion into cells. Transport studies in *E. coli* indicate that $N^{14}CO^-$ uptake involves an energy-dependent, saturable transporter with a K_m of 400 μM and a V_{max} of 4.4 nmol min^{-1} 10^9 $cells^{-1}$. CynT was initially implicated as the cyanate permease (46). But as it is now known that CynT is a soluble, cytoplasmic CA, its role in the observed intracellular accumulation of $N^{14}CO^-$ likely reflects the trapping of cyanate-derived $^{14}CO_2$, as $H^{14}CO_3^-$, within the cells (17). Since these studies were carried out, CynX has been recognized through amino acid sequence similarity to be a member of the major facilitator superfamily of transport proteins (36). However, an *E. coli* mutant defective in *cynX* was found to metabolize cyanate in a manner similar to the wild-type strain (18). Consequently, if CynX is a cyanate permease, there may be multiple pathways for NCO^- uptake in *E. coli*. Similarly, the absence of *cynX* homologs in cyanobacteria suggests the occurrence of an alternate path for cyanate transport in these organisms. Thus, there appear to be fundamental differences in the molecular components required to support cyanate metabolism in *Synechococcus* sp. strain UTEX625 and *E. coli*.

In the present study, we have used radiochemical and mass spectrometric techniques to investigate the transport of cyanate by cyanobacteria and to follow the fate of cyanate-derived CO_2 during metabolism. To determine the specificity of cyanate transport, we examined the role played by the major nutrient anion transporters in the acquisition of cyanate. We also investigated the role of an ABC-type (ATP-binding cassette) transporter that is encoded upstream of *cynS* and forms a putative operon (*cynABDS*) in *S. elongatus* strain PCC7942 and *Synechococcus* sp. strain PCC6301 but is absent in *Synechocystis* sp. strain PCC6803 (19, 20). Classification of this ABC transporter as a cyanate permease is based primarily on the proximity of *cynABD* to *cynS* (19, 20), but it is annotated as an NO_3^- or HCO_3^- transporter due to the high degree of amino acid sequence similarity between CynA and the respective periplasmic binding proteins NrtA and CmpA (29). The hypothesis that the C_i transport systems of cyanobacteria are essential to support ongoing cyanate metabolism was tested in a mutant lacking CO_2-HCO_3^- transport capability.

MATERIALS AND METHODS

Strains and growth conditions. The unicellular cyanobacteria *Synechococcus* sp. strain UTEX 625 (University of Texas Culture Collection, Austin TX; also known as *Synechococcus* sp. strain PCC6301), *S. elongatus* strain PCC7942, and *Synechocystis* sp. strain PCC6803 (Pasteur Culture Collection, Paris, France) were grown photoautotrophically in BG11 medium containing 17.5 mM $NaNO_3$. The presence of NO_3^- ensured that cyanase was fully induced (19). Cells were grown either under C_i limitation in standing culture, where diffusion of atmospheric CO_2 was the sole means of CO_2 delivery, or under high-C_i growth conditions where CO_2 was supplied by gassing buffered {25 mM 1,3-bis[Tris(hydroxymethyl)-methylamino[propane [BTP], pH 8 } cell suspensions with sterile air containing 5% (vol/vol) CO_2 at 200 ml min^{-1} (8). The *cynA* and *cynS* mutants of *S. elongatus* strain PCC7942 were grown in the presence of kanamycin (10 μg ml^{-1}), spectinomycin (40 μg ml^{-1}), or ampicillin (100 μg ml^{-1}). The Δ*chpX* Δ*chpY* mutant of *S. elongatus* strain PCC7942 (52) was kindly provided by G. D. Price (Australian National University) and was grown in the presence of kanamycin (12 μg ml^{-1}) and chloramphenicol (5 μg ml^{-1}). *E. coli* DH5α (Gibco-BRL) was grown on Luria-Bertani medium (38) and supplemented with ampicillin (100 μg ml^{-1}) or spectinomycin (50 μg ml^{-1}), when appropriate.

Insertional inactivation of *cynA* and *cynS*. Targeted mutants of *S. elongatus* strain PCC7942 were constructed by homologous recombination using antibiotic resistance cassettes to disrupt the coding sequences of the *cynA* and *cynS* genes.

Nonreplicating, pUC19-based plasmids containing either *cynA* or *cynS* (20) were cut with a restriction endonuclease at a unique ClaI or unique BglII site present within the midportion of the respective genes. The *nptII* gene, conferring kanamycin resistance, was ligated into the restricted site within *cynA* while the *aadA* gene, conferring spectinomycin resistance, was ligated into the restricted site within *cynS*. The resulting plasmids pP12::ORF440 (Amp^r Kan^r::*cynA*) and pXH::ORF146 (Amp^r Spt^r::*cynS*) were propagated in *E. coli* DH5α, purified, and transformed into *S. elongatus* strain PCC7942 using the method described by Laudenbach and Grossman (26). Transformants recovered from BG11 plates were maintained initially in the dark and then at low light (10 μmol photons m^{-2} s^{-1}; 400 to 700 nm) on 5% (vol/vol) CO_2 in air at 30°C and supplemented with 5 mM sodium thiosulfate along with the appropriate selective antibiotic (10 μg ml^{-1} kanamycin or 40 μg ml^{-1} spectinomycin). Transformants were serially streaked on fresh plates three times to encourage complete segregation. Mutants arising from homologous recombination between plasmid and *cynA* or *cynS* were recovered by replica plating and identified as colonies that were ampicillin sensitive. Genomic DNA was subsequently isolated (25) from putative, homozygous mutants and analyzed by Southern hybridization (38) to confirm the presence and location of the insert.

Database queries. Homologs of the *S. elongatus* strain PCC7942 CynA, CynS, CmpA, and NrtA proteins were identified by searching the NCBI database (National Center for Biotechnology Information, http://www.ncbi.nlm.nih.gov/) with the resident BLASTp program (1) using proteins AAB58736, AAB02940, YP_400505, and YP_400256, respectively, as individual queries. Phylogenetic trees were constructed using the TreeView program from multiple protein sequence alignments generated by Clustal X (48).

Preparation of cells. Cells (4 to 6 μg of chlorophyll [Chl] ml^{-1}) used for transport and physiological studies were harvested in mid-log phase, washed three times by centrifugation, and suspended in C_i- and Na^+-free 25 mM BTP–23.5 mM HCl buffer to a final density of 7 to 18 μg of Chl ml^{-1}. All experiments were conducted at 30°C and pH 8 to 8.3. The [Chl] of cell suspensions was measured spectrophotometrically at 665 nm after extraction in methanol (8).

O_2 evolution and chlorophyll *a* fluorescence yield. Photosynthetic O_2 evolution was measured in a Clarke-type electrode (Hansatech, Norfolk, United Kingdom) (8). Chl *a* fluorescence quenching was measured with a pulse amplitude modulation fluorometer (PAM 101; H. Walz, Effeltrich, Germany) as described previously (6). In both of the *Synechococcus* strains used, the extent of Chl *a* fluorescence quenching is directly proportional to the magnitude of the intracellular C_i pool (6). Fluorescence was, therefore, used as a surrogate to continuously monitor the formation and dissipation of the C_i pool in real time. Fluorescence quenching was expressed as a percentage of the variable fluorescence, F_V^*, such that $F_V^* = F_M^* - F_O$, where F_M is the maximum fluorescence yield and F_O is the instantaneous low-fluorescence yield (6).

Mass spectrometry (MS) and measurement of dissolved gas fluxes. The concentrations of $^{16}O_2$, $^{12}CO_2$, $^{13}CO_2$, and $^{14}CO_2$ (*m/z* values of 32, 44, 45, and 46, respectively) dissolved in reaction media or cell suspensions or arising from the metabolism of cyanate were measured using a magnetic sector MS (model MM 14-80 SC; VG Gas Analysis, Middlewich, United Kingdom,) (30). The membrane-covered inlet to the MS was inserted into a port in the side of a transparent, temperature-controlled reaction vessel to allow direct measurements of dissolved gas concentrations over time. The response of the instrument was calibrated by the addition of known concentrations of $^{16}O_2$, $K_2{}^{12}CO_3$, $K_2{}^{13}CO_3$, or $NaH^{14}CO_3$. The content of the reaction vessel was isolated from the atmosphere using a Plexiglass stopper fitted with a dual O-ring. A capillary bore in the stopper facilitated the addition of reagents to the cell suspension.

Cell suspensions in the reaction vessel were illuminated with a tungsten-halogen projector lamp (300 μmol of photons m^{-2} s^{-1}; 400 to 700 nm). Simultaneous measurements of CO_2 and O_2 fluxes and Chl *a* fluorescence yield were obtained by placing the convergent end of the four-armed fiber optic bundle of the fluorometer at the surface of the MS reaction vessel at a 90° angle to the white light source.

Radiochemical analysis of NCO^-, HCO_3^-, and CO_2 transport. Transport and intracellular accumulation were assayed using the silicone fluid filtering centrifugation technique with $N^{14}CO^-$, $H^{14}CO_3^-$, or $^{14}CO_2$ as substrate, essentially as described by Miller et al. (32). To determine the level of acid-stable products of photosynthesis and the acid-labile intracellular pool of NCO^- or C_i, the cell samples were subsequently processed as described by Espie et al. (10). Intracellular concentrations of NCO^- or C_i were calculated using an internal cellular water volume of 49 μl mg^{-1} of Chl (9).

Four variations on the transport assay protocol were used. With method A, cells were incubated in the light (300 μmol of photons m^{-2} s^{-1}; 400 to 700 nm) in the O_2-electrode chamber and allowed to deplete the medium of C_i, as indicated by the cessation of O_2 evolution. A cell sample (100 μl) was then removed and placed into a 400-μl microcentrifuge tube containing 100 μl of silicone fluid (middle layer, silicone oils AR20:AR200 at 1.75:1 (vol/vol); Wacker Chemie, Munich, Germany) and 100 μl of terminating solution (bottom layer, 2 M KOH in 10% [vol/vol] methanol). The tube was placed in a Beckman microcentrifuge E, illuminated from above (300 μmol of photons m^{-2} s^{-1}) for a further 1 min, and the experiment was started by the addition of $KO^{14}CN$ to the cells using a 10-μl Hamilton syringe. Uptake was stopped at timed intervals by centrifuging (1 min at 12,500 × g) the cells through the silicone fluid and into the terminating solution. In method B, when $N^{14}CO^-$ accumulation was measured in mutant cells or when long-term uptake assays were conducted, $KO^{14}CN$ was introduced directly into the O_2-electrode chamber. Then, under constant illumination, 100-μl samples were removed and layered on top of the silicone fluid/termination solution contained in microcentrifuge tubes. The experiment was terminated as above. For method C, another approach was used in experiments to evaluate the effect of HCO_3^- on NCO^- transport and the effect of NCO^- on HCO_3^- transport. In these experiments, the silicone fluid was overlaid with 50 μl of buffer containing $KO^{14}CN$ + $NaHCO_3$ or KOCN + $NaH^{14}CO_3$. The headspace was flushed with N_2. Cells (50 μl) depleted of C_i were then introduced into the microcentrifuge tubes in such a way as to create an N_2-filled gap between the cell suspension and the reaction buffer. The sealed tubes (six at once) were then placed in the microcentrifuge and illuminated for 1 min. To start the experiments, the cell suspensions and reaction buffers were rapidly mixed by briefly (for less than 1 s) engaging the drive of the microcentrifuge. The uptake experiments were terminated as above. For method D, when the effect of NCO^- on $^{14}CO_2$ transport was determined, NCO^- and $^{14}CO_2$ were added in rapid sequence to cells already in a microcentrifuge tube. Uptake was terminated after 10 s as described above. The $^{14}CO_2$ was created by adding $NaH^{14}CO_3$ to 10 mM phthalic acid buffer, pH 4.

KOCN and C_i contamination. Reagent grade KOCN was obtained from BDH Chemicals (Toronto, Canada) and was crystallized three times from a water-ethanol mixture prior to use (21). $KO^{14}CN$ was obtained from Dupont Canada (Mississauga), and $KO^{13}CN$ was from MSD Isotopes (Montreal). Stock solutions were made by dissolving crystallized KOCN in C_i-free water and by dissolving $KO^{14}CN$ or $KO^{13}CN$ in C_i-free 25 mM BTP buffer, pH 8. At pH 8, virtually all the KOCN existed in the form of the NCO^- anion (pK_a of HOCN is 3.7 at 27°C) (27) and slowly decomposed (0.01% h^{-1}) forming CO_2 and NH_3. The level of contaminant $^{12}CO_2$, $^{13}CO_2$, or $^{14}CO_2$ present in KOCN solutions, "C_i-free" buffers, and other solutions was routinely determined by MS. Equilibrium C_i concentrations were subsequently calculated for the experimental temperature and pH as described by Stumm and Morgan (42). Typically, freshly crystallized and freshly prepared 1 mM KOCN stock solutions contained 7.1 ± 2 μM $^{12}C_i$ (n = 7) while 1 mM $KO^{14}CN$ contained 6.5 ± 1.8 μM $^{14}C_i$ (n = 7), and 1 mM $KO^{13}CN$ contained 86.5 ± 9.7 μM $^{13}C_i$ (n = 7). These values increased over time. The $KO^{14}CN$ stock solutions contained less than 2% acid-stable material, and its presence was corrected for in calculations. In some experiments, the level of C_i contamination in solutions could be reduced to near-zero by first allowing cells to photosynthetically deplete the reaction medium. But in all cases, appropriate corrections were made to the specific activities of radiochemicals and to concentrations of reactants to account for the presence of contaminant C_i.

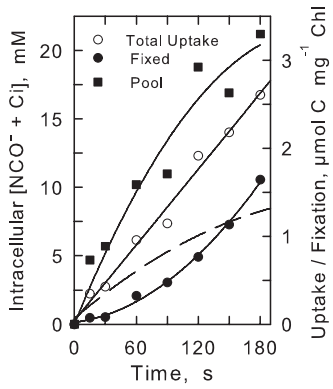

FIG. 1. Time course (180 s) of NCO^- uptake in the light for *Synechococcus* sp. strain UTEX 625 standing culture cells provided with 1 mM $KO^{14}CN$, as determined by method A. Shown are total uptake (○), the acid-stable products of C-fixation (●), and the acid-labile intracellular pool of NCO^- + C_i (■). Data are the average of three replicates ±10.4% (maximum). Also shown (dashed line) is the calculated intracellular pool of NCO^- corrected for intracellular C_i.

Cyanate is relatively stable in alkaline solution (hydrolysis rate of 0.01% h^{-1}) but rapidly decomposes to CO_2 and NH_3 below about pH 4.5 (27). Consequently, unreacted $N^{14}CO^-$ was removed from samples by acidification and driving off the resulting $^{14}CO_2$ by evaporation.

Nucleotide sequence accession numbers. The nucleotide sequence of the *cynABDS* region determined in this study has been deposited in the GenBank database at NCBI under accession numbers AF001333 and U59481.

RESULTS

Cyanate uptake and the fate of cyanate-derived ^{14}C. Figure 1 shows a typical time course of ^{14}C uptake by *Synechococcus* sp. strain UTEX 625 (PCC6301) cells provided with 1 mM $KO^{14}CN$. The intracellular ^{14}C was found in two major fractions: an acid-stable fraction composed of metabolic intermediates and an acid-labile fraction consisting of unreacted $N^{14}CO^-$ and $^{14}C_i$. Over the course of the experiment (180 s), the intracellular acid-labile pool of ^{14}C rose to about 21 mM.

Interpretation of cyanate uptake experiments (Fig. 1 and 2) is complicated by the presence of $^{14}C_i$ which invariably contaminated the $KO^{14}CN$ (7 to 25 μM/1 mM). This $^{14}C_i$ was undoubtedly transported rapidly into the cells by the high-affinity C_i transport systems and fixed by the Calvin cycle enzyme ribulose-1,5-bisphospahate carboxylase, thereby contributing to both the acid-labile and acid-stable fractions (9, 12, 31, 32). In fact, nearly all the ^{14}C fixed during the uptake experiments (Fig. 1) entered the acid-stable fraction via the photosynthetic carbon reduction cycle as evidenced by the fact that darkness, DCMU (3[3,4-dichlorophenyl]-1,1-dimethylurea), and the Calvin cycle inhibitor glycolaldehyde reduced ^{14}C incorporation by 98%, 98%, and 94%, respectively (Table 1). Over the course of 25-min experiments (Fig. 2), 18 to 26% of the total added C (as KOCN) was found in the acid-stable fraction. This level of incorporation exceeded the $^{14}C_i$ available in $KO^{14}CN$ solutions by at least 36-fold. During the short-

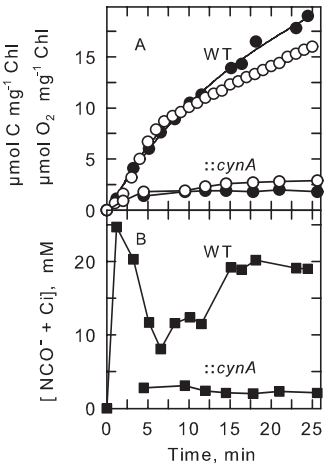

FIG. 2. Typical time course (25 min) of NCO^- uptake and utilization by *S. elongatus* PCC7942 wild type (WT) and the *cynA* mutant (::*cynA*). Cells grown in standing culture with low C_i concentrations were provided with 1 mM $KO^{14}CN$ in the light. Uptake and accumulation of ^{14}C was determined as described in method B. (A) Simultaneous measurements of cyanate-dependent CO_2 fixation (●) and O_2 evolution (○) for the wild type and the *cynA* mutant. (B) Intracellular accumulation of acid-labile $NCO^- + C_i$ (■) for the wild type and the *cynA* mutant (::*cynA*).

term experiments (Fig. 1), ^{14}C incorporation exceeded the available $^{14}C_i$ by fourfold, indicating that most of the ^{14}C found in the acid-stable fraction was derived from the ^{14}C originally present in $KO^{14}CN$.

The incorporation of ^{14}C into acid-stable products initially lagged behind the accumulation of the acid-labile internal pool of ^{14}C (Fig. 1). But as this pool increased in size so, too, did the rate of C incorporation, approaching a steady-state rate as the internal pool approached a maximum. The dynamics of these two fractions were indicative of a precursor-product relationship in which the acid-labile C (NCO^- and C_i) was first transported and accumulated within the cells and, subsequently, incorporated into acid-stable products of photosynthesis.

Cyanate supported light-dependent O_2 evolution at a linear rate for about 10 min, after which the rate declined to a lower steady-state rate (Fig. 2). The decline in the rate of O_2 evolution was paralleled by a decline in C-fixation and coincided in time with a decrease in the internal $NCO^- + C_i$ pool (Fig. 2). With time, the internal pool stabilized at a new steady-state level leading to a lower steady-state rate of cyanate-dependent O_2 evolution and C-fixation. Biphasic time courses of O_2 evolution were commonly observed when cells were provided with KOCN exceeding about 100 μM. A near 1:1 stoichiometry was found between added KOCN, O_2 evolution, and CO_2 fixation (Fig. 2) (30), consistent with the complete decomposition of cyanate to NH_3 and CO_2 and subsequent fixation of CO_2 into acid-stable products of photosynthesis.

The ability of *Synechococcus* sp. UTEX 625 to utilize cyanate-derived CO_2 to support photosynthesis was affected by the level of C_i experienced during growth. For cells grown in standing culture (low C_i concentration, approximately 20 μM), with air bubbling (intermediate C_i concentration, approximately 180 μM), or bubbling with 5% CO_2 (high C_i concentration), analysis of cyanate response curves indicated $K_{0.5}$ (the substrate concentration that yields one-half the maximum rate) (NCO^-) values for O_2 evolution of 0.34 ± 0.04, 0.43 ± 0.13, and 0.70 ± 0.05 mM and maximum rates of 138 ± 10, 187 ± 34, and 233 ± 43 μmol O_2 mg^{-1} of Chl h^{-1} (± standard deviation; $n = 3$), respectively. Since growth on C_i also affects the level of induction of the CCM (5), the data suggest a possible role for the CCM in modulating cyanate utilization.

Active transport and accumulation of NCO^-. Cyanate uptake was stimulated by light and inhibited by DCMU, suggesting that photosynthetic electron transport may be involved in energizing or activating NCO^- transport (Table 1). An acid-labile pool of C was also formed in the presence of glycolaldehyde, indicating that uptake was not strictly tied to the photosynthetic metabolism of cyanate. Oxalate, a membrane-impermeant inhibitor of both *E. coli* and cyanobacterial cyanase (3, 30), had little effect on either the acid-labile or acid-stable fractions (Table 1), indicating that cyanase was absent from the periplasm. This finding is consistent with previous biochemical studies which show cyanase activity in the soluble, cytoplasmic fraction of cell lysates (19, 30). Consequently, NCO^- and/or HOCN must permeate the inner membrane prior to decomposition.

In order to distinguish between $N^{14}CO^-$ uptake and accumulation and $^{14}C_i$ uptake and accumulation (Fig. 1), we conducted a series of experiments in the presence of unlabeled $^{12}C_i$ (Table 2). Through dilution with $^{12}C_i$, the specific activity of the $^{14}C_i$ present as a contaminant in $KO^{14}CN$ solutions was reduced by up to 1,000-fold, effectively eliminating the contribution of $^{14}C_i$ uptake to the intracellular acid-labile pool. Table 2 shows that the initial rate (20 s) of ^{14}C uptake by cells presented with 1 mM $KO^{14}CN$ was 48% or 49% of the control value in the presence of 2 or 5 mM $^{12}C_i$, respectively. Similarly, the internal pool was reduced to 45% or 46% of the control value, while ^{14}C-fixation declined to 47% to 42% of the control. Slightly larger decreases in the rate of uptake and intracellular accumulation were observed over 120-s time intervals while ^{14}C-fixation declined by as much as 75% (Table 2). Consequently, we estimated that 40% to 45% of the total acid-labile intracellular pool of ^{14}C was comprised of $N^{14}CO^-$. Based on this estimate, the intracellular concentration of cyanate would be expected to be about 2.7 mM at 20 s, 6.3 mM at 120 s (Table 2), and 8.4 mM at 180 s (Fig. 1). This latter value is 8.4-fold higher than the initial concentration of KOCN provided to the cells. Assuming a membrane potential of

TABLE 1. Characterization of NCO^- uptake and metabolism in *Synechococcus* sp. strain UTEX 625

Experimental conditions[a]	$N^{14}CO^-$ uptake (% of control)	^{14}C fixation (% of control)
Light (control)	100	100
Dark	6.3	2.4
Light + 25 μM DCMU	7.9	2.2
Light + 15 mM glycolaldhyde	59.1	5.6
Light + 15 mM oxalate	88	99.7
Light + 1 mM ethoxyzolamide	39	32.3

[a] NCO^- uptake and C fixation were measured by the silicone fluid filtering centrifugation technique using method A. Cells grown in standing culture were incubated with 1 mM $KO^{14}CN$ for 2 min in BTP/HCl buffer, pH 8.0, containing 25 mM NaCl at 30°C and illuminated at 300 μmol m^{-2} s^{-1}. Data are the average of 5 experiments in triplicate ±6.5%.

TABLE 2. Effect of [^{12}Ci] on $N^{14}CO^-$ transport by *Synechococcus* sp. strain UTEX 625 grown in standing culture[a]

Experimental condition (with 1 mM $KO^{14}CN$)	% of control value at 20 s			% of control value at 2 min		
	$N^{14}CO^-$ uptake	Pool	^{14}C fixation	$N^{14}CO^-$ uptake	Pool	^{14}C fixation
0 mM $KHCO_3$	100	100[b]	100[c]	100	100[d]	100[e]
2 mM $KHCO_3$	48.2 ± 9.3	45.4 ± 16.2	47.5 ± 21.6	38.4 ± 15.2	41.0 ± 12.9	24.9 ± 10.6
5 mM $KHCO_3$	49.4 ± 7.3	46.4 ± 19.3	42.9 ± 12.2	39.6 ± 14.6	41.5 ± 18.7	30.4 ± 19.7

[a] Values were determined using method C in BTP-HCl buffer, pH 8, containing 25 mM NaCl. Light was supplied at 300 μmol of photons m^{-2} s^{-1}. Data are the average of seven experiments ± standard deviations.
[b] Control value, 6.0 ± 2.0 mM.
[c] Control value, 0.06 μmol of C mg^{-1} Chl.
[d] Control value, 11.0 ± 7.0 mM.
[e] Control value, 0.23 μmol of C mg^{-1} Chl.

−0.12 V (37), the electrochemical potential for NCO^- was calculated to be 16.6 kJ mol^{-1} (−0.63 V), indicating that a component of NCO^- uptake involved carrier-mediated, active transport.

Transport specificity. The reduction in ^{14}C accumulation in the presence of $^{12}C_i$ (Table 2) may also indicate a competition between C_i and NCO^- during transport. Consequently, the possibility that NCO^- transport was gratuitously mediated via one of the C_i transport systems or one of the major nutrient anion transport systems was tested in a series of competition experiments in the presence of CO_2, HCO_3^-, NO_3^-, NO_2^-, Cl^-, PO_4^{2-}, or SO_4^{2-} (Fig. 3 and 4).

Physiologically, C_i transport in *Synechococcus* sp. strain UTEX 625 (PCC6301) and *S. elongatus* strain PCC7942 is comprised of an active, Na^+-dependent HCO_3^- uptake activity, an active Na^+-independent HCO_3^- uptake activity, and high- and low-affinity active CO_2 uptake activities (6, 9, 12, 31). These transport activities are thought to involve the membrane proteins SbtA, CmpABCD, NdhF3/NdhD3/ChpY, and NdhF4/NdhD4/ChpX, respectively (reviewed in reference 5). If one or more of these transporters is involved in NCO^- transport, then NCO^- must also be an inhibitor of C_i transport activity. Figure 3A and B show that neither Na^+-independent HCO_3^- transport nor Na^+-dependent HCO_3^- transport was inhibited by up to a 24-fold excess of KOCN. However, in cells grown with low C_i concentrations in standing culture and with high C_i concentrations, CO_2 transport was reduced by up to 50% with 1 mM KOCN (Fig. 3C). Thus, NCO^- transport may occur through the CO_2 transport system. The fact that NCO^- is an isoelectronic structural analog of CO_2 supports this view. However, although $^{14}CO_2$ transport assays were conducted rapidly, the $^{12}CO_2$ generated from the decomposition of cyanate (Fig. 4) may also have contributed to the apparent inhibition of $^{14}CO_2$ transport. Thus, the involvement of the CO_2 transport systems in NCO^- transport requires further analysis (see below).

The involvement of nitrate/nitrite transport systems in NCO^- transport was tested in a different way. The *Synechococcus* strains grown under high-C_i conditions have a greatly reduced capacity for HCO_3^- transport and rely primarily on the low affinity CO_2 uptake system for C_i acquisition (5). Consequently, the contribution (if any) of the CO_2 transport systems to NCO^- transport can be minimized. When cells grown with high C_i concentrations were presented with $N^{13}CO^-$, a large and sustained rise in the extracellular $^{13}CO_2$ concentration was observed that was light dependent (Fig. 4). The ad-

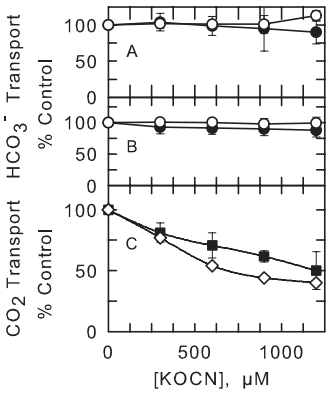

FIG. 3. Effect of KOCN on HCO_3^- and CO_2 transport in *Synechococcus* sp. strain UTEX 625 cells grown in standing culture. The initial rate (20 s) of HCO_3^- transport was measured (method C) at substrate concentrations of 50 μM (●) and 250 μM (○) in pH 8 buffer to determine the effect of increasing [KOCN] on Na^+-independent HCO_3^- transport in the presence of 100 μM NaCl (A) or Na^+-dependent HCO_3^- transport in the presence 30 mM NaCl (B). (C) The initial rate (10 s) of CO_2 transport (■) was measured at 10 μM in the presence of 100 μM NaCl (method D). Also shown is the effect of KOCN on CO_2 transport in cells grown under high-C_i conditions(◇). The data are the average of six determinations ± standard deviations.

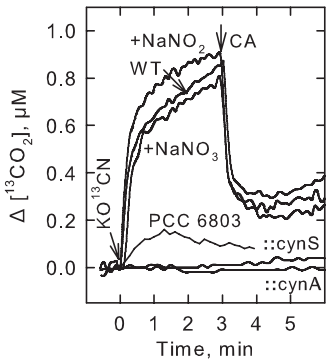

FIG. 4. KOCN-dependent CO_2 efflux by cells grown under high-CO_2 conditions. Illuminated wild-type (WT) *S. elongatus* PCC7942 cells were provided with 1 mM $KO^{13}CN$, and the efflux of $^{13}CO_2$ was followed by MS over time in the absence or presence of 25 mM $NaNO_3$ or $NaNO_2$. Bovine CA was added to the suspension to illustrate that CO_2 was the C_i species arising in the cell suspensions. Also shown are the CO_2 fluxes arising from the *cynA* and *cynS* mutants and from *Synechocystis* sp. strain PCC6803 grown in high-CO_2 concentrations.

dition of bovine CA to cell suspensions reduced the [$^{13}CO_2$], indicating that it was CO_2 and not HCO_3^- that exited the cells and that the CO_2 was present at a concentration well above its chemical equilibrium with HCO_3^-. The use of KO^{13}CN as substrate confirmed that the $^{13}CO_2$ arising in the medium was derived directly from cyanate uptake and decomposition rather than from respiration or any other process (30). Consequently, in vivo cyanate uptake and decomposition can be followed in real time by measuring KOCN-dependent CO_2 efflux via MS (Fig. 4).

When *S. elongatus* strain PCC7942 was presented with KO^{13}CN in the presence of either 25 mM $NaNO_3$ or 25 mM $NaNO_2$, both the qualitative and quantitative patterns of $^{13}CO_2$ formation were very similar to the control pattern observed with cells in buffer alone (Fig. 4) or in the presence of 25 mM NaCl (not shown). Thus, neither NO_3^- nor NO_2^- interfered with the process of cyanate uptake or its decomposition to CO_2. Since the nitrate/nitrite transport systems were saturated at these levels, we conclude that these transporters were not involved in the transport of NCO^-. Similarly, neither phosphate nor sulfate affected the patterns of KOCN-dependent CO_2 efflux (not shown).

In cells grown under low-C_i conditions, the steady-state rate of KOCN-dependent O_2 evolution in the light was also not substantially reduced by the presence of nutrient anions. Measured rates (100 μM KOCN; $n = 3$) in the presence of 25 mM NO_3^-, NO_2^-, Cl^-, PO_4^{2-}, and SO_4^{2} were 92.0%, 97.1%, 104%, 94.1%, and 89.2% of the control value (25 mM BTP, pH 8). Collectively, the data indicated that none of the major inorganic anion transport systems played a significant role in the active transport of NCO^-.

***cynS* is required but not sufficient to promote the metabolism of exogenous NCO^-.** Southern hybridization analysis of ClaI-digested DNA from *S. elongatus* strain PCC7942 wild-type and the *cynS* mutant was carried out using a 187-bp EcoR1-BglII restriction fragment from *cynS* as the probe. A single hybridization signal of approximately 7.0 kb was obtained from DNA from the *cynS* mutant compared to a 5.0-kb band from wild-type DNA (not shown). The 2-kb difference corresponded well to the expected insertion of the Spt^r cassette into *cynS* and indicates that only a single disrupted copy of *cynS* was present in the genome of the *S. elongatus* strain PCC7942 *cynS* mutant.

Previous studies have shown that targeted interruption of *cynS* in *S. elongatus* strain PCC7942 results in the loss of intracellular cyanase activity (19). Consistent with this is the observation that our *cynS* mutant was unable to utilize exogenously supplied KOCN to support photosynthetic O_2 evolution (Fig. 5A). The inability of the *cynS* mutant to utilize NCO^- was not related to a defect in the photosynthetic utilization of cyanate-derived CO_2 since it grew photoautotrophically in a normal fashion under low-C_i conditions and responded in a comparable manner to wild-type cells when supplied with 25 μM C_i. The *cynS* mutant was also able to form and retain a large internal pool of C_i when provided with exogenous 25 μM C_i, as judged by an increase in Chl *a* fluorescence quenching (Fig. 5B). The addition of KOCN also elicited substantial fluorescence quenching (43% of F_V* after 5 min) in wild-type cells which corresponded to an internal C_i pool of about 28 to 30 mM (6). KOCN-dependent fluorescence

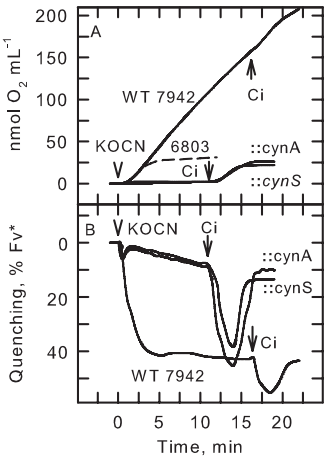

FIG. 5. Measurements of KOCN-dependent O_2 evolution (A) and Chl *a* fluorescence quenching (B) in *S. elongatus* PCC7942 wild-type (WT) cells and the *cynA* and *cynS* mutants. Cells grown under low-C_i conditions were allowed to deplete the medium of C_i in the light. Cells were then provided with 1 mM KOCN, and O_2 evolution and Chl *a* fluorescence quenching were measured simultaneously over time. Once a steady state was achieved, C_i-dependent O_2 evolution and Chl *a* fluorescence quenching were also measured following the addition of 25 μM C_i to the cell suspensions. Also shown in panel A is the response of *Synechocystis* sp. strain PCC6803 to the addition of 1 mM KOCN.

quenching preceded the onset of steady-state photosynthesis, consistent with an initial uptake and subsequent decomposition of cyanate to form an internal pool of CO_2. These responses to KOCN were completely absent in the *cynS* mutant (Fig. 5B), as was the rise in CO_2 concentration following KOCN addition to cells grown under high-Ci conditions (Fig. 4). The disruption of *cynS* thus led to the loss of intracellular cyanase activity (19) and to an inability to metabolize exogenous cyanate in vivo.

Although the cyanobacterium *Synechocystis* sp. strain PCC6803 also expresses a high level of cyanase activity when grown with nitrate as its N source (19), the wild-type cells were unable to utilize exogenous cyanate to support O_2 evolution in the light (Fig. 5A). In addition, *Synechocystis* sp. strain PCC6803 cells grown under high-Ci conditions failed to create the sustained rise in extracellular CO_2 concentration in the light that was characteristic of cyanate decomposition (Fig. 4), in spite of the presence of abundant and functional cyanase (19). These data suggest that molecular components beyond *cynS* are required to facilitate the metabolism of exogenous cyanate in the two *Synechococcus* strains and that some or all of these components are lacking naturally or are not expressed in *Synechocystis* sp. strain PCC6803.

***cynA* is required for cyanate transport.** Immediately upstream of *cynS* in *S. elongatus* strain PCC7942 and *Synechococcus* sp. strain PCC6301, but not *Synechocystis* sp. strain PCC6803, is a three-gene cluster (GenBank accession numbers AF001333 and U59481) initially designated as *orf440*, *orf263*, and *orf289* and later renamed *cynA*, *cynB*, and *cynD*, respectively (19, 20). The *cyn* genes are all transcribed in the same direction (*cynA* to *cynS*) and are separated by 9, 3, and 10 nucleotides, respectively. Putative ribosome binding sites are located 7 to 10 bp upstream of start codons in all but *cynD* (16).

A potential transcription termination sequence is located downstream of *cynS* (20) while an NtcA-dependent promoter is located upstream of *cynA* between −334 and −293 (19) (GenBank accession number AB005890). Sequence analysis, therefore, predicts that *cynA*, *cynB*, *cynD*, and *cynS* form an operon. This view is supported by Northern hybridization analysis which indicates that both *cynA* (20) and *cynS* (19, 20) are present on a transcript approximately 4.3 kb in size.

The deduced amino acid sequences of CynA, CynB, and CynD show significant sequence identity to proteins that are members of the ABC-type superfamily of membrane transport proteins (19, 20). The protein encoded by *cynB* has characteristics typical of the integral membrane permease component of the transport system while CynD contains ATP-binding motifs characteristic of the peripheral membrane component involved in the energization of transport (19, 20). CynA, a putative periplasmic binding protein, has a high degree of amino acid similarity to its paralogs NtrA (46%) and CmpA (45%). The latter two periplasmic proteins are known to bind NO_3^-/NO_2^- and HCO_3^-, respectively (29, 34). Thus, CynA may be a monovalent anion binding protein.

To determine if the *cynABDS* operon is involved in cyanate transport, we characterized a *S. elongatus* strain PCC7942 *cynA* mutant, which was created by interrupting the *cynA* gene with a Kan^r cassette. Southern hybridization analysis of PstI-digested DNA from *S. elongatus* strain PCC7942 wild type and the *cynA* mutant strain, using a 687-bp PstI-ClaI restriction fragment from *cynA* as the probe, revealed the presence of a single disrupted copy of *cynA* in the genome of the mutant (not shown). The *cynA* mutant was unable to carry out KOCN-dependent O_2 evolution or KOCN-dependent Chl *a* fluorescence quenching, although the mutant was capable of typical wild-type C_i-dependent O_2 evolution and C_i-dependent Chl *a* fluorescence quenching (Fig. 5). Similarly, *cynA* mutant cells grown with high C_i concentrations did not evolve CO_2 when presented with KOCN (Fig. 4), indicating that the lesion in *cynA* had disrupted their ability to utilize exogenous cyanate. Transport assays (Fig. 2) revealed a marked decline in intracellular $N^{14}CO^-$ accumulation and the absence of sustained ^{14}C fixation in the light compared to wild-type cells. In these experiments, sampling of the *cynA* mutant was begun 5 min after the addition of 2 mM $KO^{14}CN$. This allowed the mutant sufficient time to fix contaminating $^{14}C_i$ into acid-stable products, as judged by O_2 evolution and fluorescence measurements. Consequently, direct measurements of the acid-labile intracellular $N^{14}CO^-$ pool were possible (Fig. 2B). The average intracellular concentration of NCO^- in the *cynA* mutant was 2.1 ± 1.1 mM ($n = 6$) after a 5-min exposure and 3.1 ± 1.9 mM ($n = 6$) after a 10-min exposure. In comparison, wild-type *S. elongatus* strain PCC7942 accumulated a total pool of 27.1 ± 8.1 mM ($n = 8$) after 5 min and 37.1 ± 11.1 mM ($n = 8$) after 10 min. From these data, internal concentrations of NCO^- of 12.2 and 16.7 mM, respectively, were calculated assuming that 45% of the measured pool in wild-type cells was free NCO^-. Consequently, the level of NCO^- accumulation in the *cynA* mutant is at least fivefold lower than in wild-type cells. Calculations using the Henderson-Hasselbach equation indicate that about one-half of the observed accumulation in the *cynA* mutant was accounted for by the diffusion of HOCN into the cells and its passive equilibration with NCO^-. Thus, the ability of the *cynA* mutant to transport and concentrate NCO^- is severely impaired.

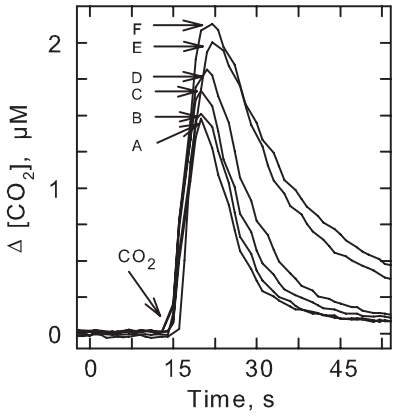

FIG. 6. Effect of KOCN on CO_2 transport. *S. elongatus* PCC7942 *cynA* mutant cells grown under low-C_i conditions were placed in the reaction chamber attached to the MS and allowed to equilibrate (25 mM BTP-HCl buffer, pH 8, at 30°C) in the light (300 μmol of photons m^{-2} s^{-1}) in the presence of KOCN. CO_2 transport was initiated by adding 3.5 μM CO_2 to the reaction vessel, and its concentration was followed over time. The difference between the curves obtained in the light (A, 0 mM KOCN, maximum uptake) and the dark (F, no uptake) was taken as a measure of CO_2 transport. The effect of 1, 3, 5, or 10 mM KOCN (B, C, D, and E) on CO_2 transport are also shown.

Inhibition of CO_2 transport by NCO^-. Since the *cynA* mutant does not generate CO_2 from NCO^-, this mutant was used to further examine KOCN inhibition of CO_2 transport (Fig. 3) using an MS assay (11). Pure CO_2 was introduced into the reaction cuvette, and its disappearance was followed over time (Fig. 6). The differences between the curves obtained in the light and the dark were a consequence of cellular uptake and a measure of CO_2 transport (11). In contrast to wild-type cells (Fig. 3C), 1 mM KOCN had little effect on CO_2 transport in the mutant (Fig. 6). However, at 10 mM KOCN, CO_2 transport was reduced by nearly 90%. Although high concentrations of KOCN inhibited CO_2 transport in the mutant, the lack of an effect at 1 mM indicated that the inhibition by 1 mM KOCN on $^{14}CO_2$ transport in wild-type cells (Fig. 3C) was due mainly to competition with $^{12}CO_2$ generated from the decomposition of cyanate. NCO^-, therefore, is an inhibitor of the CO_2 uptake system but is not a transported substrate.

The role of the CCM and the C_i transporters in cyanate metabolism. HCO_3^- is also required by cyanase as a substrate, and it seems reasonable to assume that the CCM of *S. elongatus* strain PCC7942 plays a direct role in its provision in the light, particularly given that the net rate of cyanate decomposition may reach 230 μmol mg^{-1} of Chl h^{-1}. The role of the internal C_i pool in promoting cyanate metabolism was tested using the Δ*chpX* Δ*chpY* mutant of *S. elongatus* strain PCC7942 grown on 5% CO_2. As this mutant lacks CO_2 transport capabilities and HCO_3^- transport is repressed by growth under high-C_i conditions, it has little or no ability to concentrate C_i internally (52). Consequently, diffusion of C_i largely controls the size of the internal C_i pool in the Δ*chpX* Δ*chpY* mutant both in the light and dark. In these experiments (Fig. 7), we controlled the size of the C_i pool by imposing diffusion gradients between C_i-free cells and the medium through the provi-

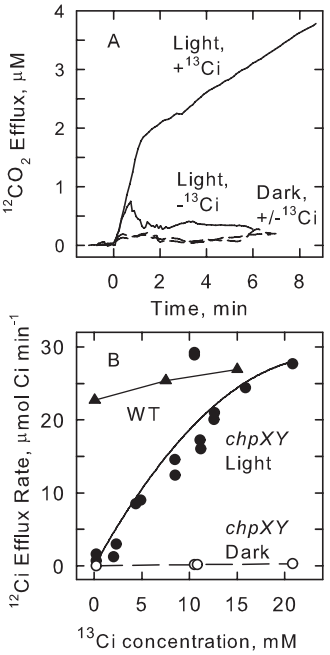

FIG. 7. Involvement of the cyanobacterial CCM in cyanate metabolism. (A) Time course of KOCN-dependent $^{12}CO_2$ efflux in the light (solid lines) and dark (dashed lines). *S. elongatus* strain PCC7942 Δ*chpX* Δ*chpY* cells grown on 5% CO_2 were suspended in 100 mM EPPS (*N*-[2-hydroxyethyl]piperazine-*N*′-[3-propanesulfonic acid]) buffer, pH 8, and incubated in the light or dark for 5 min in the reaction cuvette, in the absence and presence of 10 mM $NaH^{13}CO_3$ ($^{13}C_i$). The experiment was started by the addition of 1 mM KOCN, and $^{12}CO_2$ efflux was measured over time by MS. (B) Dependence of $^{12}C_i$ efflux rate on $^{13}C_i$ concentration. The average rate of $^{12}C_i$ efflux, at a constant cell density (7.5 μg of Chl *a* ml^{-1}), was calculated from $^{12}CO_2$ efflux measurements over an 8-min interval as a function of $^{13}C_i$ concentration for Δ*chpX* Δ*chpY* (*chpXY*) cells in the light (●) and dark (○) provided with 1 mM KOCN. Also shown (dashed line and ▲) is the dependence on $^{13}C_i$ concentration of $^{12}CO_2$ efflux in *S. elongatus* PCC7942 wild-type (WT) cells grown under low-C_i conditions.

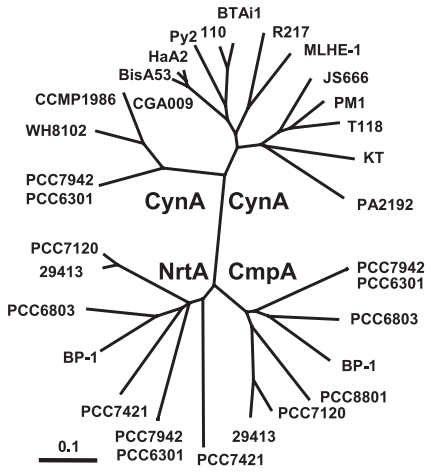

FIG. 8. Unrooted phylogenetic tree illustrating the relationship between CynA proteins identified from bacterial sources and NrtA and CmpA from cyanobacteria. Cyanobacterial species are as follows: *S. elongatus* PCC7942, *Synechococcus* sp. strain PCC6301, *Synechocystis* sp. strain PCC6803, *Thermosynechococcus elongatus* BP-1, *Cyanothece* sp. strain PCC8801, *Nostoc* sp. strain PCC7120, *Anabaena variabilis* ATCC 29413, *Gloeobacter violaceus* PCC7421, *Synechococcus* sp. strain WH8102, and *P. marinus* CCMP1986. Other organisms are *Rhodopseudomonas palustris* strains CGA009, BisA53, and HaA2; *Xanthobacter autotrophicus* Py2; *Bradyrhizobium japonicum* USDA 110; *Bradyrhizobium* sp. strain BTAi1; *Roseovarius* sp. strain R217; *Alkalilimnicola ehrlichei* MLHE-1; *Polaromonas* sp. strain JS666; *Rubrivivax gelatinosus* PM1; *Rhodoferax ferrireducens* T118; *Methylobacillus flagellatus* KT; and *Pseudomonas aeruginosa* PA2192. Organisms are represented on the figure generally by the strain designation or culture collection number.

sion of various concentrations of exogenous $^{13}C_i$. Following equilibration between the medium and the cells, we measured the average rate of decomposition of 1 mM KOCN as $^{12}C_i$ efflux over a 6- to 8-min period in the light and dark. A typical time course is shown for the Δ*chpX* Δ*chpY* mutant in the presence and absence of 10 mM $NaH^{13}CO_3$ (Fig. 7A). The data confirm that cyanate transport was light dependent and demonstrated that the rate of cyanate decomposition was dependent upon and limited by the size of the internal C_i pool, approaching a maximum rate beyond 20 mM C_i (Fig. 7B). In wild-type cells grown under low-C_i conditions, a 20 mM C_i pool is readily formed in the light when the external C_i concentration is about 20 μM (6). Consequently, the C_i that contaminated buffers and KOCN in our experiments was a sufficient source of substrate for the CCM to provide an internal HCO_3^- concentration that was able to support a near-maximum rate of KOCN decomposition without supplementing the buffer with C_i (Fig. 7B). Supplementing the buffer with 7.5 or 15 mM $NaH^{13}CO_3$ resulted in only a modest increase in the rate of cyanate decomposition by wild-type cells grown under low-Ci conditions. This result is consistent with the internal HCO_3^- concentration being at a near-saturating level for cyanase when the external C_i concentration is extremely low.

There was no specific requirement for either the Na^+-dependent or Na^+-independent HCO_3^- transport systems to form the C_i pool as growth under high-C_i conditions, which repressed these activities (5, 12), did not prevent cyanate uptake, decomposition (Fig. 4), or KOCN-dependent O_2 evolution. Similarly, ethoxyzolamide, a CO_2 transport inhibitor, did not completely prevent $KO^{14}CN$ accumulation and ^{14}C- fixation in cells grown under low-C_i conditions (Table 1) or KOCN-dependent CO_2 efflux (not shown). We conclude that an internal C_i pool in the millimolar range (Fig. 7), independent of the actual means by which it is formed, is a corequisite for KOCN metabolism in *S. elongatus* strain PCC7942. However, under normal physiological conditions (0.001 to 5 mM C_i), one or more of the C_i transport systems is required to actively create an internal C_i pool if cyanate metabolism is to proceed at a significant rate (Fig. 7B).

Occurrence of *cynABDS* among *Bacteria*. A search of the NCBI database using the BLASTp program identified 98 bacterial strains (out of 598 as of 22 July 2006) bearing a protein with amino acid sequence similarity to CynS of *S. elongatus* strain PCC7942. These included 12 of 24 cyanobacterial strains. Gene clusters encoding putative ABC-type transporters were also found adjacent to *cynS* in 17 strains, including four cyanobacteria, *S. elongatus* strain PCC7942, *Synechococcus* sp. strain PCC6301, *Prochlorococcus marinus* strain CCMP1986, and *Synechococus* sp. strain WH8102 (Fig. 8) (14,

43). Additional BLASTp searches using *S. elongatus* strain PCC7942 CynA as the query revealed that all 17 of the putative periplasmic substrate-binding proteins found encoded near *cynS* were highly related (E values less than 10^{-85}) and more closely related to one another than to NrtA or CmpA (Fig. 8). Similarly, when CynB from *S. elongatus* strain PCC7942 was the query, the permease components most similar to it were those that were encoded by permease components adjacent to *cynS* (E values less than 10^{-59}) (data not shown). However, this type of association broke down in the case of CynD, the ATP-binding protein that energizes transport. Since the substrate specificity of individual ABC-type transporters is determined by the binding protein and the permease subunits, while energization is a more generic function, it is likely that the newly identified *cynABDS*-like operons encode components for cyanate transport and degradation. Most of these ABC-transporters have previously been annotated as nitrate transporters and/or as simply possessing a twin-arginine signal sequence. In addition to the four cyanobacteria, *cynABDS*-like operons were found in seven strains of the *Alphaproteobacteria*, four strains of *Betaproteobacteria*, and two strains of *Gammaproteobacteria* (Fig. 8). Most of these strains (11/17) were obligate or facultative chemo- or photoautotrophs. The remaining strains consisted of heterotrophs that oxidized a range of organic compounds and a single obligate methylotroph.

DISCUSSION

A model for cyanate metabolism. The results of our investigation indicate that the transport and decomposition of exogenously supplied cyanate by strains of the freshwater cyanobacterium *Synechococcus* depend upon the products of the *cynABDS* operon and the biophysical activity of the CCM in a light-dependent manner. With the exception of *cynS*, the molecular components required to support the transport and cellular decomposition of cyanate are distinct from the components encoded by the *cynTSX* operon of *E. coli* and thus constitute a novel mechanism that facilitates the assimilation of C and N from cyanate. Indeed, it is likely that an *E. coli*-like system for cyanate metabolism would be deleterious in cyanobacteria because the cytosolic CA component would circumvent the operation of parts of the CCM.

Inactivation of *cynA*, which encodes the periplasmic binding protein of a putative multicomponent ABC-type transporter, results in the loss of active cyanate transport and the ability to decompose NCO^- to CO_2 and NH_3. Similarly, inactivation of *cynS*, which codes for a cytosolic cyanase, yields a mutant that is also unable to decompose cyanate. As a result, both mutants lack cyanate-dependent O_2 evolution and CO_2 efflux. An additional novel aspect of cyanate metabolism in cyanobacteria is its dependence on light and photosynthetic electron transport. This dependence was multifaceted and traced to the light dependence of both cyanate transport and C_i transport. Presumably, ATP derived from photophosphorylation is used to energize cyanate transport through the membrane-bound ATP-binding protein CynD. Although oxidative phosphorylation also yields ATP, there is little active cyanate transport in the dark. These results suggest that cyanate transport activity is regulated by an additional step beyond energy supply or simple kinetic control mechanisms associated with substrate concentration. The codependence of cyanate and C_i transport on light further suggests that the transporters may be controlled by a common activation/deactivation mechanism. Such a mechanism ensures that the transport of a potential toxin into the cells is coupled with the means to rapidly degrade it. However, ongoing C_i transport is not a prerequisite for the activation of NCO^- transport as evidenced by the fact that the Δ*chpX* Δ*chpY* mutant of *S. elongatus* strain PCC7942 was able to decompose exogenous NCO^- when provided with an adequate supply of internal HCO_3^-, which was acquired through CO_2 diffusion (Fig. 7).

The role of the CCM in cyanate metabolism. The rate of cyanate decomposition depends on the size of the internal HCO_3^- pool, which in turn is controlled by the activity of the CCM in the light (Fig. 7). In the absence of a functional CCM, cyanate decomposition was severely retarded at external C_i concentrations usually experienced during growth and points to the fact that CO_2 diffusion is normally inadequate to supply intracellular HCO_3^- for cyanase. Coupling of cyanate decomposition to the CCM is a unique strategy for HCO_3^- acquisition that distinguishes *S. elongatus* strain PCC7942 from *E. coli* and, potentially, autotrophic cyanate metabolism from heterotrophic cyanate metabolism, which relies on the combined action of cyanase and CA. CA, which is crucial for the provision of HCO_3^- in the cytosol of *E. coli*, is confined to carboxysomes in the *Synechococcus* strains and functions in the opposite direction to supply CO_2 for photosynthetic fixation (5, 39). A direct role for cyanobacterial CA in the trapping of HCO_3^- in the cytosol for cyanase is not indicated by virtue of the massive efflux of cyanate-derived CO_2 that occurs in cells grown under high-C_i conditions. The high capacity of the cyanobacterial CCM to concentrate HCO_3^- internally over a wide range of external C_i concentrations is an important factor which circumvents the limitation imposed by external C_i concentration and CO_2 diffusion on the cellular capacity for cyanate decomposition and is a key reason why *Synechococcus* strains are able to have a 20-fold higher capacity for cyanate decomposition compared to *E. coli* (30).

The dependence of cyanate decomposition on the activity of the CCM also facilitates the assimilation of cyanate-derived CO_2 through the photosynthetic carbon reduction cycle. This is most evident in cells grown in low C_i concentrations where a high-affinity CCM is fully induced. In these cells, CO_2 efflux is substantially diminished (30), and this is reflected in a $K_{0.5}$ (NCO^-) value for photosynthetic cyanate utilization that is twofold lower compared to cells grown in high C_i concentrations. The superior retention of cyanate-derived CO_2 by cells grown in low C_i concentrations coincides with the up-regulation of the high-affinity CO_2 uptake system (51) that is predominantly localized to the thylakoid membranes. Presumably, CO_2 loss from the cytoplasm is curtailed through its conversion to HCO_3^- by the light-driven action of the NdhF3/NdhD3/ChpY complex rather than carboxysome-localized CA. The trapped HCO_3^- then contributes to the overall internal pool available for photosynthetic fixation. Cyanate-derived CO_2 that is lost from cells will undoubtedly be recovered by the C_i transport systems and eventually fixed, as evidenced by the 1:1 stoichiometry between added NCO^- and CO_2 fixation (O_2 evolution). In the short term, the proportion of CO_2 that is lost from the cell to that which is retained will depend on the level

of induction of the CCM and the capacity of the cell for CO_2 fixation.

Cyanate transport. The high degree of amino acid sequence similarity between CynA and its paralogs NrtA and CmpA suggests that CynA may also perform similar transport functions in cellular metabolism. Consequently, the notion that CynABD acts as an NO_3^-/NO_2^- transporter or HCO_3^- transporter in *S. elongatus* strain PCC7942 was investigated along with the hypothesis that native NO_3^-/NO_2^- transporters or HCO_3^- transporters accept NCO^- as an alternative substrate. In competition assays (Fig. 4), however, neither excess NO_3^- nor NO_2^- (as well as Cl^-, PO_4^{2-}, or SO_4^{2-}) impaired the release of cyanate-derived CO_2 from whole cells, indicating that these anions did not interfere with the initial uptake of NCO^-, as would be expected for alternative substrates of a common transporter. It seems unlikely, therefore, that CynABD is an NO_3^-/NO_2^- transporter that gratuitously transports NCO^-. For the same reason, it is also unlikely that NCO^- transport in *S. elongatus* strain PCC7942 is mediated by the bona fide NO_3^-/NO_2^- transporter, NrtABCD, as suggested for *Azotobacter chroococcum* (33).

The potential role of the HCO_3^- and CO_2 transport systems in NCO^- transport proved to be more difficult to unravel due to the nonenzymatic interconversion between HCO_3^- and CO_2, the presence of multiple C_i transporters, the contamination of labeled KOCN solutions with labeled C_i, the slow but spontaneous hydrolysis of cyanate-forming C_i, and the rapid enzymatic decomposition of NCO^- that yielded a large quantity of CO_2 within seconds of addition. ^{14}C-bicarbonate transport assays (Fig. 3) revealed that NCO^- did not compete with $H^{14}CO_3^-$ for uptake, consistent with a lack of involvement of CmpABCD or SbtA in the transport of NCO^- by *S. elongatus* strain PCC7942. The roughly 50 to 60% reduction in ^{14}C accumulation observed in $N^{14}CO^-$ transport assays (Table 2) when cells were supplied with excess $^{12}C_i$ can be ascribed to the competitive elimination by $H^{12}CO_3^-$ of the transport of $H^{14}CO_3^-$ that contaminates $KO^{14}CN$ solutions rather than a direct inhibition of NCO^- transport by HCO_3^-, since a reciprocal inhibition of HCO_3^- transport by NCO^- did not occur. The fact that the effect of "cold" HCO_3^- on $N^{14}CO^-$ transport saturated at 2 mM suggests that CynABD is not an HCO_3^- transporter since high HCO_3^- concentrations should eliminate NCO^- transport.

Inhibitor studies have provided evidence both for and against a role for the CO_2 transport system in NCO^- transport (Fig. 3 and 6). While 1 mM NCO^- appeared to inhibit $^{14}CO_2$ transport in wild-type *S. elongatus* strain PCC7942 cells, 1 mM NCO^- had no effect on CO_2 transport in the *cynA* mutant, as judged by MS. The most likely explanation for this apparent discrepancy is that cyanate-derived $^{12}CO_2$ released from wild-type cells during transport experiments competed with $^{14}CO_2$ for uptake, thereby reducing the internal concentration of ^{14}C. Since the *cynA* mutant does not decompose cyanate, cyanate-derived $^{12}CO_2$ competition is not a complicating factor in determining whether or not cyanate inhibits CO_2 transport. Thus, these results lead us to conclude that cyanate is not a substrate of the CO_2 transport systems. This conclusion is also consistent with the observed inability of *Synechocystis* sp. strain PCC6803 to decompose externally supplied cyanate to CO_2 and NH_3 (Fig. 4), in spite of possessing a functional CO_2 transport system to potentially deliver NCO^- to the cytosol for cyanase.

The inability of *Synechocystis* sp. strain PCC6803 to decompose externally supplied cyanate in the light as well as the inability of the *S. elongatus* strain PCC7942 Δ*chpX* Δ*chpY* mutant to decompose cyanate in the dark at high internal HCO_3^- concentrations (Fig. 7) indicates that the diffusive entry of HOCN contributes minimally to the gross uptake of cyanate. Thus, the collective data demonstrate that the *Synechococcus* strains are able to actively transport and concentrate NCO^- through a specific pathway that involves CynA and, therefore, CynB and CynD. We are now in the process of determining if CynA is an NCO^- binding protein. The detailed kinetics of cyanate transport have yet to be resolved, due to the technical difficulties of separating the initial flux of NCO^- from the flux and reflux of CO_2 and HCO_3^-. It is clear, however, that a transient net flux of up to 230 μmol mg^{-1} of Chl h^{-1} is possible as this is the maximum steady-state rate of cyanate-dependent O_2 evolution. In our experiments, the ratio of $[NCO^-]_{in}/[NCO^-]_{out}$ was in the range of 8 to 10 at 1 mM NCO^-. These estimates were complicated by the need to apply a substantial correction for $^{14}C_i$ accumulation and are subject to future refinement. Nevertheless, the data indicate that NCO^- was concentrated above the level expected from diffusion alone.

cynABDS-like operons are present in a diverse range of cyanobacteria and proteobacteria, including the globally important oceanic cyanobacteria *Synechococcus* sp. strain WH8102 and *P. marinus* strain CCMP1986 (Fig. 8). It seems likely that the HCO_3^- required for NCO^- decomposition is provided by the CCM of these two organisms. A CCM has yet to be identified in autotrophic proteobacteria, such as *Rhodopseudomonas palustris* and *Bradyrhizobium* sp. strain BTAi1, which possess *cynABDS*-like operons. Interestingly, these organisms lack carboxysomes, a hallmark of the cyanobacterial CCM. Thus, it is possible that they may employ their own unique strategy for HCO_3^- acquisition or utilize a cytosolic CA. Alternatively, NCO^- degradation may be restricted to naturally occurring high C_i environments where CO_2 diffusion could play a role. This latter route for HCO_3^- acquisition may also be of particular importance for the heterotrophs which possess *cynABDS*-like operons.

Physiological role. One experimentally verified role for CynABDS in cellular metabolism is to provide a vehicle for the transport and decomposition of exogenous cyanate. Since the *Synechococcus* strains readily assimilate cyanate-derived CO_2 (Fig. 1 and 2) and NH_3 (30), CynABDS permits the utilization of cyanate as a niche source of C and N for growth. CynS alone cannot fulfill this metabolic role. Thus, CynABDS may be legitimately included as an input branch to the major C and N assimilatory pathways in cyanobacteria. The relatively high capacity for NCO^- transport and decomposition may reflect a metabolic strategy for rapid utilization from environments where NCO^- is only sporadically available and has a short half-life. Utilization of NCO^- broadens the range of available C and N sources and may provide a small advantage over organisms that can only assimilate NH_3, particularly in oligotrophic environments where C_i and N sources limit growth (13, 14, 43). In other environments such as industrial waste waters, relatively high concentrations of NCO^- are available, pro-

duced by bacterial consortia (heterotrophs and autotrophs) that are actively degrading thiocyanate (41, 50). Here, the opportunistic utilization of cyanate by cyanobacteria may reflect their participation in thiocyanate metabolism. We are currently investigating the possibility that cyanobacteria may also directly metabolize thiocyanate.

ACKNOWLEDGMENT

This work was supported by grants from the Natural Sciences and Engineering Research Council of Canada to G.S.E. Part of this work was conducted by G.S.E. at the Research School of Biological Sciences, The Australian National University.

We sincerely thank G. D. Price and M. R. Badger for the provision of research facilities and for access to the *S. elongatus* strain PCC7942 Δ*chpX* Δ*chpY* mutant. We also thank Ben Long, The Australian National University, and A. G. Miller, St. Francis Xavier University, for valuable discussions.

REFERENCES

1. **Altschul, S. F., T. L. Madden, A. A. Schaffer, J. Zhang, Z. Zhang, W. Miller, and D. J. Lipman.** 1997. Gapped BLAST and PSI-BLAST: a new generation of protein database search programs. Nucleic Acids Res. **25:**3389–3402.
2. **Anderson, P. M.** 1980. Purification and properties of the inducible enzyme cyanase. Biochemistry **19:**2882–2888.
3. **Anderson, P. M., W. V. Johnson, J. A. Endrizzi, R. M. Little, and J. J. Korte.** 1987. Interaction of mono- and dianions with cyanase: evidence for apparent half-site binding. Biochemistry **26:**3938–3943.
4. **Anderson, P. M., Y. C. Sung, and J. A. Fuchs.** 1990. The cyanase operon and cyanate metabolism. FEMS Microbiol. Rev. **87:**247–252.
5. **Badger, M. R., G. D. Price, B. M. Long, and F. J. Woodger.** 2006. The environmental plasticity and ecological genomics of the cyanobacterial CO_2 concentrating mechanism. J. Exp. Bot. **57:**249–265.
6. **Crotty, C. M., P. N. Tyrrell, and G. S. Espie.** 1994. Quenching of chlorophyll *a* fluorescence in response to Na^+-dependent HCO_3^- transport-mediated accumulation of inorganic carbon in the cyanobacterium *Synechococcus* UTEX 625. Plant Physiol. **104:**785–791.
7. **Dorr, P. K., and C. J. Knowles.** 1989. Cyanide oxygenase and cyanase activities of *Pseudomonas fluorescens* NCIMB 11764. FEMS Microbiol. Rev. **60:**289–294.
8. **Espie, G. S., and D. T. Canvin.** 1987. Evidence for Na^+-independent HCO_3^- uptake by the cyanobacterium *Synechococcus leopoliensis*. Plant Physiol. **84:** 125–130.
9. **Espie, G. S., and R. A. Kandasamy.** 1992. Na^+-independent HCO_3^- transport and accumulation in the cyanobacterium *Synechococcus* UTEX 625. Plant Physiol. **98:**560–568.
10. **Espie, G. S., A. G. Miller, and D. T. Canvin.** 1988. Characterization of the Na^+ requirement in cyanobacterial photosynthesis. Plant Physiol. **88:**757–763.
11. **Espie, G. S., A. G. Miller, and D. T. Canvin.** 1989. Selective and reversible inhibition of active CO_2 transport by hydrogen sulfide in a cyanobacterium. Plant Physiol. **91:**387–394.
12. **Espie, G. S., A. G. Miller, R. A. Kandasamy, and D. T. Canvin.** 1991. Active HCO_3^- transport in cyanobacteria. Can. J. Bot. **69:**936–944.
13. **Flores, E., and A. Herrero.** 2005. Nitrogen assimilation and nitrogen control in cyanobacteria. Biochem. Soc. Trans. **33:**164–167.
14. **Garcia-Fernandez, J. M., N. Tandeau de Marsac, and J. Diez.** 2004. Streamlined regulation and gene loss as adaptive mechanisms in *Prochlorococcus* for optimized nitrogen utilization in oligotrophic environments. Microbiol. Mol. Biol. Rev. **68:**630–638.
15. **Guilloton, M., and F. Karst.** 1987. Isolation and characterization of *Escherichia coli* mutants lacking inducible cyanase. J. Gen. Microbiol. **133:**645–653.
16. **Guilloton, M. B., G. S. Espie, and P. M. Anderson.** 2002. What is the role of cyanase in plants? Rev. Plant Biochem. Biotechnol. **1:**57–79.
17. **Guilloton, M. B., J. J. Korte, A. F. Lamblin, J. A. Fuchs, and P. M. Anderson.** 1992. Carbonic anhydrase in *Escherichia coli*: a product of the cyn operon. J. Biol. Chem. **267:**3731–3734.
18. **Guilloton, M. B., A. F. Lamblin, E. I. Kozliak, M. Gerami-Nejad, C. Tu, D. Silverman, and J. A. Fuchs.** 1993. A physiological role for cyanate-induced carbonic anhydrase in *Escherichia coli*. J. Bacteriol. **175:**1443–1451.
19. **Harano, Y., I. Suzuki, S. I. Maeda, T. Kaneko, S. Tabata, and T. Omata.** 1997. Identification and nitrogen regulation of the cyanase gene from the cyanobacteria *Synechocystis* sp. strain PCC 6803 and *Synechococcus* sp. strain PCC 7942. J. Bacteriol. **179:**5744–5750.
20. **Jalali, F.** 1997. Molecular cloning, insertional inactivation and characterization of the cyanate lyase gene from the cyanobacterium *Synechococcus* PCC 7942. M.S. thesis. University of Toronto, Mississauga, Ontario, Canada.
21. **Johnson, W. V., and P. M. Anderson.** 1987. Bicarbonate is a recycling substrate for cyanase. J. Biol. Chem. **262:**9021–9025.
22. **Kozliak, E. I., J. A. Fuchs, M. B. Guilloton, and P. M. Anderson.** 1995. Role of bicarbonate/CO_2 in the inhibition of *Escherichia coli* growth by cyanate. J. Bacteriol. **177:**3213–3219.
23. **Kozliak, E. I., M. B. Guilloton, J. A. Fuchs, and P. M. Anderson.** 2000. Bacterial carbonic anhydrases, p. 547–565. *In* W. R. Chegwidden, N. D. Carter, and Y. H. Edwards (ed.), The carbonic anhydrases: new horizons. Birkhauser Verlag, Basil, Switzerland.
24. **Kozliak, E. I., M. B. Guilloton, M. Gerami-Nejad, J. A. Fuchs, and P. M. Anderson.** 1994. Expression of proteins encoded by the *Escherichia coli* cyn operon: carbon dioxide-enhanced degradation of carbonic anhydrase. J. Bacteriol. **176:**5711–5717.
25. **Kuhlemeier, C. J., and G. A. van Arkel.** 1987. Host-vector systems for gene cloning in cyanobacteria. Methods Enzymol. **153:**199–215.
26. **Laudenbach, D. E., and A. R. Grossman.** 1991. Characterization and mutagenesis of sulfur-regulated genes in a cyanobacterium: evidence for function in sulfate transport. J. Bacteriol. **73:**2739–2750.
27. **Lister, M. W.** 1955. Some observations on cyanic acid and cyanates. Can. J. Biochem. **33:**426–440.
28. **Little, R. M., and P. M. Anderson.** 1987. Structural properties of cyanase: denaturation, renaturation, and role of sulfhydryls and oligomeric structure in catalytic activity. J. Biol. Chem. **262:**10120–10126.
29. **Maeda, N., G. D. Price, M. R. Badger, C. Enomoto, and T. Omata.** 2000. Bicarbonate binding activity of the CmpA protein of the cyanobacterium *Synechococcus* sp. strain PCC 7942 involved in active transport of bicarbonate. J. Biol. Chem. **275:**20551–20555.
30. **Miller, A. G., and G. S. Espie.** 1994. Photosynthetic metabolism of cyanate by the cyanobacterium *Synechococcus* UTEX 625. Arch. Microbiol. **162:**151–157.
31. **Miller, A. G., G. S. Espie, and D. T. Canvin.** 1991. Active CO_2 transport in cyanobacteria. Can. J. Bot. **69:**925–935.
32. **Miller, A. G., G. S. Espie, and D. T. Canvin.** 1988. Active transport of CO_2 by the cyanobacterium *Synechococcus* UTEX 625: measurement by mass spectrometry. Plant Physiol. **86:**677–683.
33. **Muñoz-Centeno, M. C., A. Paneque, and F. J. Cejudo.** 1996. Cyanate is transported by the nitrate permease in *Azotobacter chroococcum*. FEMS Microbiol. Lett. **137:**91–94.
34. **Omata, T., Y. Takahashi, O. Yamaguchi, and T. Nishimura.** 2002. Structure, function and regulation of the cyanobacterial high-affinity bicarbonate transporter, BTC1. Funct. Plant Biol. **29:**151–159.
35. **Palenik, B., B. Brahamsha, F. Larimer, M. Land, L. Hauser, P. Chain, J. Lamerdin, W. Regals, E. Allen, J. McCarren, I. Paulsen, A. Dufresne, F. Partensky, E. Webb, and J. Waterbury.** 2003. The genome of a motile marine *Synechococcus*. Nature **424:**1037–1042.
36. **Pao, S. S., I. Paulsen, and M. H. Saier.** 1998. Major facilitator superfamily. Microbiol. Mol. Biol. Rev. **62:**1–34.
37. **Ritchie, R. J.** 1991. Membrane potential and pH control in the cyanobacterium *Synechococcus* R-2 (*Anacystis nidulans*) PCC 7942. Plant Physiol. **137:** 409–418.
38. **Sambrook, J., E. F. Fritch, and T. Maniatis.** 1989. Molecular cloning: a laboratory manual, 2nd ed. Cold Spring Harbor Laboratory Press, Cold Spring Harbor, NY.
39. **So, A. K. C., and G. S. Espie.** 2005. Cyanobacterial carbonic anhydrases. Can. J. Bot. **83:**721–734.
40. **So, A. K. C., M. E. John-McKay, and G. S. Espie.** 2002. Characterization of a mutant lacking carboxysomal carbonic anhydrase from the cyanobacterium *Synechocystis* PCC6803. Planta **214:**456–467.
41. **Sorokin, D. Y., T. P. Tourova, A. M. Lysenko, and J. G. Kuenen.** 2001. Microbial thiocyanate utilization under highly alkaline conditions. Appl. Environ. Microbiol. **67:**528–538.
42. **Stumm, W., and J. J. Morgan.** 1981. Aquatic chemistry, 2nd ed. John Wiley & Sons, Toronto, Canada.
43. **Su, Z., F. Mao, P. Dam, H. Wu, V. Olman, I. T. Paulsen, B. Palenik, and Y. Xu.** 2006. Computational inference and experimental validation of the nitrogen assimilation network in cyanobacterium *Synechococcus* sp. WH 8102. Nucleic Acids Res. **34:**1050–1065.
44. **Sung, Y. C., and J. A. Fuchs.** 1988. Characterization of the cyn operon in *Escherichia coli* K12. J. Biol. Chem. **263:**14769–14775.
45. **Sung, Y. C., and J. A. Fuchs.** 1992. The *Escherichia coli* K-12 cyn operon is positively regulated by a member of the *lysR* family. J. Bacteriol. **174:**3645–3650.
46. **Sung, Y. C., and J. A. Fuchs.** 1989. Identification and characterization of a cyanate permease in *Escherichia coli* K-12. J. Bacteriol. **171:**4674–4678.
47. **Taussig, A.** 1960. The synthesis of the enzyme cyanase in *E. coli*. Biochim. Biophys. Acta **44:**510–519.
48. **Thompson, J. D., T. J. Gibson, F. Plewniak, F. Jeanmougin, and D. J. Higgins.** 1997. The Clustal X windows interface: flexible strategies for multiple sequence alignment aided by quality analysis tools. Nucleic Acids Res. **25:**4876–4882.
49. **Walsh, M. A., Z. Otwinowski, A. Perrakis, P. M. Anderson, and A.**

Joachimiak. 2000. Structure of cyanase reveals that a novel dimeric and decameric arrangement of subunits is required for formation of the enzyme active site. Struct. Fold Des. **8:**505–514.
50. **Wood, A. P., D. P. Kelly, I. R. McDonald, S. L. Jordan, T. D. Morgan, S. Khan, J. C. Murrell, and E. Borodina.** 1998. A novel, pink-pigmented facultative methylotroph, *Methylbacterium thiocyanatum* sp. nov., capable of growth on thiocyanate or cyanate as sole nitrogen source. Arch. Microbiol. **169:**148–158.
51. **Woodger, F. J., M. R. Badger, and G. D. Price.** 2003. Inorganic carbon limitation induces transcripts encoding components of the CO_2-concentrating mechanism in *Synechococcus* sp. PCC7942 through a redox-independent pathway. Plant Physiol. **133:**2069–2080.
52. **Woodger, F. J., M. R. Badger, and G. D. Price.** 2005. Sensing of inorganic carbon limitation in *Synechococcus* PCC7942 is correlated with the size of the internal inorganic carbon pool and involves oxygen. Plant Physiol. **139:** 1959–1969.
53. **Youatt, J. B.** 1954. Studies on the metabolism *Thiobacillus thiocyanooxidans*. J. Gen. Microbiol. **11:**139–140.